

Neutrino Nucleus Reactions based on New Shell Model Hamiltonians

Toshio Suzuki*

*Department of Physics, College of Humanities and Sciences, Nihon University
Sakurajosui 3-25-40, Setagaya-ku, Tokyo 156-8550, Japan*

Satoshi Chiba

*Advanced Science Research Center, Japan Atomic Energy Agency
2-4 Shirakata-shirane, Tokai, Naka-gun, Ibaraki 319-1195, Japan*

Takashi Yoshida

National Astronomical Observatory of Japan, Mitaka, Tokyo 181-8588, Japan

Toshitaka Kajino

*National Astronomical Observatory of Japan, Mitaka, Tokyo 181-8588, Japan
Department of Astronomy, Graduate School of Science,
University of Tokyo, Bunkyo-ku, Tokyo 113-0033, Japan*

Takaharu Otsuka

*Department of Physics, University of Tokyo, Hongo, Bunkyo-ku, Tokyo 113-0033, Japan
Center for Nuclear Study, University of Tokyo, Hongo, Bunkyo-ku, Tokyo 113-0033, Japan
RIKEN, Hirosawa, Wako-shi, Saitama 351-0198, Japan*

(Dated: October 10, 2018)

A new shell model Hamiltonian for p -shell nuclei which properly takes into account important roles of spin-isospin interactions is used to obtain cross sections of neutrino- ^{12}C reactions induced by decay-at-rest (DAR) neutrinos as well as supernova neutrinos. Branching ratios to various decay channels are calculated by the Hauser-Feshbach theory. Neutrino- ^4He reactions are also investigated by using recent shell model Hamiltonians. The reaction cross sections are found to be enhanced for both ^{12}C and ^4He compared with previous calculations. As an interesting consequence of this, a possible enhancement of the production yields of light elements, ^7Li and ^{11}B , during supernova explosions is pointed out.

PACS numbers: 25.30.-c, 21.60.Cs

I. INTRODUCTION

A recent progress in shell model calculations, which properly takes into account important roles of spin-isospin interactions, is found to lead to significant improvements in magnetic properties of nuclei [1] as well as proper shell evolution, that is, the change of magic numbers toward the drip-lines [2, 3]. An important general role of the tensor interaction is pointed out [3]. The modified Hamiltonian can explain spin properties of the p -shell nuclei such as Gamow-Teller transitions better than conventional shell model Hamiltonians. In particular, agreements between calculated and observed magnetic moments are found to be systematically improved for the p -shell nuclei [1].

Here, we study new ingredients of these developments on neutrino-nucleus reactions on ^{12}C , which are dominantly induced by Gamow-Teller and spin-dipole transitions. Charge-exchange and neutral current reactions induced by neutrinos from pion decay-at rest (DAR)

and supernova neutrinos are investigated, and comparisons are made with previous calculations [4, 5, 6]. We also study neutrino-nucleus reactions on ^4He , which are mainly induced by spin-dipole transitions. We discuss possible effects of our new neutrino-nucleus reaction cross sections on nucleosynthesis process, in particular, on light element abundances during supernova explosions.

The paper is organized as follows. In section II, we discuss tensor components of our modified interaction. Neutrino-nucleus reaction cross sections on ^{12}C and ^4He are obtained by using our new shell model Hamiltonian in section III. Astrophysical implications are discussed in section IV, and a summary is given in section V.

II. NEW SHELL MODEL HAMILTONIAN FOR p -SHELL NUCLEI

We discuss some important ingredients of our new shell model Hamiltonian for p -shell nuclei in ref. [1], where the spin-isospin flip interaction and the shell gap between the $0p_{1/2}$ and $0p_{3/2}$ orbits are enhanced in comparison to the Cohen-Kurath Hamiltonian, (8-16)2BME [7]. We will refer to this Hamiltonian as SFO hereafter.

First, we show that the dominant effect of the enhance-

*Electronic address: suzuki@chs.nihon-u.ac.jp

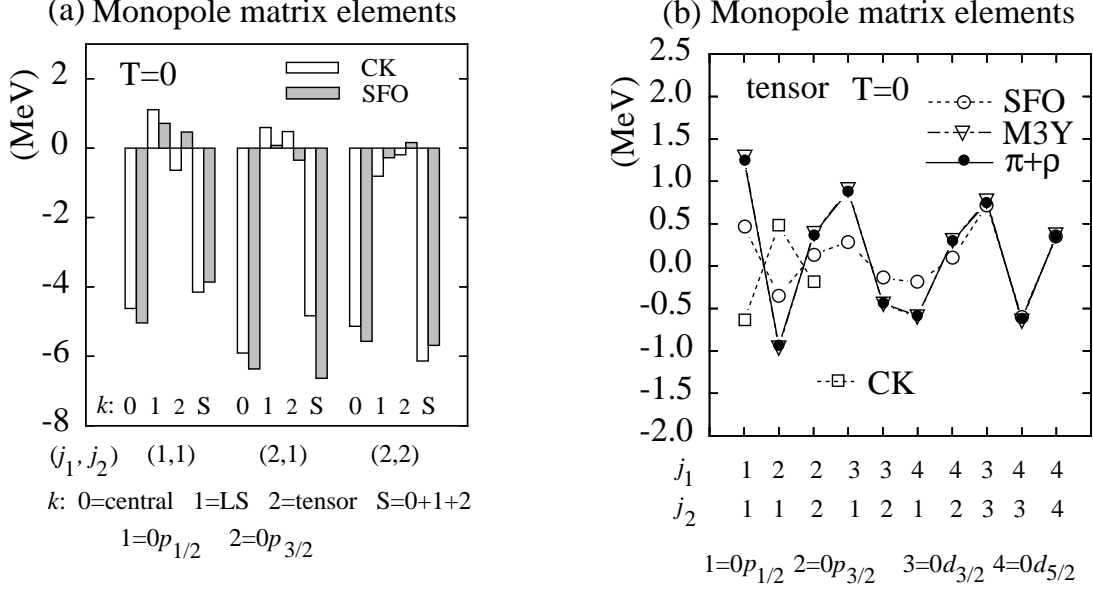


FIG. 1: (a) Monopole terms of the central ($k=0$), spin-orbit ($k=1$) and tensor ($k=2$) components of the SFO and Cohen-Kurath interactions. (b) Monopole terms of the tensor component of the SFO and Cohen-Kurath interactions as well as the $\pi + \rho$ exchange potential and the M3Y interaction.

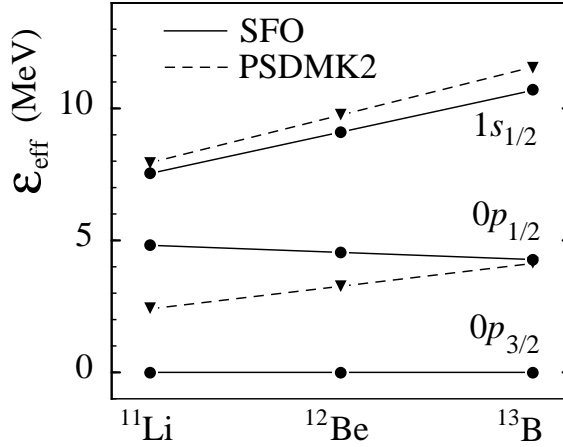


FIG. 2: Effective neutron single particle energies relative to that of the $0p_{3/2}$ orbit for $N=8$ isotones.

ment of the spin-flip two-body matrix elements in the isospin $T=0$ channel, $\langle 0p_{3/2}0p_{1/2} : JT | V | 0p_{3/2}0p_{1/2} : JT \rangle$ with $J=1, 2$, is the modification of the tensor component of the interaction. Spin-tensor decomposition of the two-body effective interactions for a specific isospin channel can be done by expanding the matrix element with those of the same orbital angular momenta [8, 9]. Each matrix element is decomposed into the central ($k=0$), spin-orbit ($k=1$) and tensor ($k=2$) components,

$$\langle ab : JT | V | cd : JT \rangle = \sum_k \langle ab : JT | V_k | cd : JT \rangle \quad (1)$$

with

$$\begin{aligned} \langle ab : JT | V_k | cd : JT \rangle &= (-1)^J (2k+1) \sum_{LL'SS'} \\ &\langle ab | LSJ \rangle \langle cd | L'S'J \rangle \left\{ \begin{matrix} L & S & J \\ S' & L' & k \end{matrix} \right\} \sum_{J'} (-1)^{J'} \\ &(2J'+1) \left\{ \begin{matrix} L & S & J' \\ S' & L' & k \end{matrix} \right\} \sum_{j'_a j'_b j'_c j'_d} \langle a'b' | LSJ' \rangle \\ &\langle c'd' | L'S'J' \rangle \langle a'b' : J'T | V | c'd' : J'T \rangle \quad (2) \end{aligned}$$

where $a = \{n_a \ell_a j_a\}$, $a' = \{n_a \ell_a j'_a\}$, and $\langle ab | LSJ \rangle =$

$$\left\{ \begin{array}{ccc} \ell_a & 1/2 & j_a \\ \ell_b & 1/2 & j_b \\ L & S & J \end{array} \right\} \hat{j}_a \hat{j}_b \hat{L} \hat{S} \text{ with } \hat{L} = 2L + 1 \text{ etc.}$$

The monopole terms of the three components

$$V_k^{j_1 j_2, M} = \frac{\sum_J (2J+1) \langle j_1 j_2 : JT | V_k | j_1 j_2 : JT \rangle}{\sum_J (2J+1)} \quad (3)$$

are shown in Fig. 1a for the p -shell matrix elements with $T=0$ for the SFO and the original Cohen-Kurath Hamiltonian. We find that the most important modification appears in the tensor components where even the signs of the matrix elements are changed. The central components of the monopole terms are also increased. Note that the total p -shell matrix elements are renormalized by a factor 0.93 [1].

The attractive (repulsive) nature of the tensor components of the monopole matrix elements with $j_1 = j_2 = 0p_{3/2}$ and $j_2 = j_1 = 0p_{1/2}$ ($j_1 = j_2 = j_1 = 0p_{3/2}$ or $j_1 = j_2 = j_1 = 0p_{1/2}$) is consistent with the general robust nature of the tensor interaction [3].

Although the magnitude of the tensor components of the monopole matrix elements of the SFO Hamiltonian is small compared with that of the pion and rho-meson ($\pi + \rho$) exchange potential with a radial cut off at 0.7 fm [10] and the M3Y interaction [11], their signs and the zigzag pattern of the monopole matrix element as a function of $j_1 - j_2$ and $j_1 - j_2$ or $j_1 - j_2$ are consistent as shown in Fig. 1b. This zigzag structure with the proper signs in the tensor monopole terms is important and essential for the proper shell evolution.

Next, we show how these important characteristics affect the behavior of the effective single particle energies. Effective neutron single particle energies for $N=8$ isotones are shown in Fig. 2. The effective single particle energy is the sum of the bare single particle energy for the ^4He core and monopole two-body matrix elements of the proton-neutron (p-n) interaction summed over occupied proton orbits outside the ^4He core. Since the tensor interaction is attractive between the proton (π) $0p_{3/2}$ orbit and neutron (ν) $0p_{1/2}$ orbit while it is repulsive between the $\pi 0p_{3/2}$ and $\nu 0p_{3/2}$ orbits, the energy gap between the $\nu 0p_{1/2}$ and $\nu 0p_{3/2}$ orbits becomes larger as the proton number gets smaller, that is, for more neutron-rich isotones. The monopole terms of the central interaction are attractive both for $j_1 = \pi 0p_{3/2}$, $j_2 = \nu 0p_{1/2}$ and $j_1 = \pi 0p_{3/2}$, $j_2 = \nu 0p_{3/2}$, and their difference has the same sign as the tensor interaction but the magnitude is smaller about by half. The monopole terms of the spin-orbit interaction work opposite to the tensor and central interactions. The proper shell evolution is not obtained in case of the original Cohen-Kurath interaction as the monopole terms of the tensor components have opposite signs compared to the SFO interaction, which results in the reduction of the energy gap between the $\nu 0p_{1/2}$ and $\nu 0p_{3/2}$ orbits in the neutron-rich side.

We shall now go on to the question of to what extent such a shell evolution is related to neutrino-nucleus reactions.

III. NEUTRINO NUCLEUS REACTIONS

A. REACTIONS ON ^{12}C INDUCED BY DAR NEUTRINOS

We showed in ref.[1] that the magnetic properties of p -shell nuclei are considerably improved, for example, in magnetic moments and Gamow-Teller transitions. Here, we study another example of spin dependent transitions, namely neutrino-nucleus reactions, which are induced mainly by excitations of Gamow-Teller and spin-dipole states.

We focus here on reactions on ^{12}C , as the Gamow-Teller transition to the ground states of ^{12}N and ^{12}B are studied quite well [1, 12]. Charge-exchange reactions as well as neutral current reactions induced by DAR neutrinos are investigated. The electron neutrinos produced from the DAR pions and the μ^+ decay have average energy of about 35 MeV with an upper limit at 52.8 MeV. The reactions are induced dominantly by the axial-vector current. Contributions from the vector current are rather small but not negligible.

The multipole expansions of the reaction cross sections induced by ν or $\bar{\nu}$ are given as follows [13],

$$\begin{aligned} \left(\frac{d\sigma}{d\Omega} \right)_{\frac{\nu}{\bar{\nu}}} &= \frac{G^2 \epsilon k}{4\pi^2} \frac{4\pi}{2J_i + 1} \left\{ \sum_{J=0}^{\infty} \{ (1 + \vec{\nu} \cdot \vec{\beta}) \right. \\ &| \langle J_f \| M_J \| J_i \rangle |^2 + [1 - \hat{\nu} \cdot \vec{\beta} + 2(\hat{\nu} \cdot \hat{q})(\hat{q} \cdot \vec{\beta})] \\ &| \langle J_f \| L_J \| J_i \rangle |^2 - \hat{q} \cdot (\hat{\nu} + \vec{\beta}) 2\text{Re} \langle J_f \| L_J \| J_i \rangle \\ &\langle J_f \| M_J \| J_i \rangle^* \} + \sum_{J=1}^{\infty} \{ [1 - (\hat{\nu} \cdot \hat{q})(\hat{q} \cdot \vec{\beta})] \\ &(| \langle J_f \| T_J^{el} \| J_i \rangle |^2 + | \langle J_f \| T_J^{mag} \| J_i \rangle |^2 \\ &\pm \hat{q} \cdot (\hat{\nu} - \vec{\beta}) 2\text{Re} \langle J_f \| T_J^{mag} \| J_i \rangle \\ &\langle J_f \| T_J^{el} \| J_i \rangle^* \} \} \end{aligned} \quad (4)$$

where $\vec{\nu}$ and \vec{k} are neutrino and lepton momenta, respectively, ϵ is the lepton energy, $\vec{q} = \vec{k} - \vec{\nu}$, $\vec{\beta} = \vec{k}/\epsilon$, $\hat{\nu} = \vec{\nu}/|\vec{\nu}|$ and $\hat{q} = \vec{q}/|\vec{q}|$.

For charge-exchange reactions, $G = G_F \cos\theta_C$ with G_F the Fermi coupling constant and θ_C the Cabbibo angle, and the lepton is electron or positron. For neutral current reactions, $G = G_F$ and the lepton is scattered neutrino. The cross section is multiplied by the Fermi function $F(Z_f, E_\ell)$ [14], where Z_f is the charge of the daughter nucleus and E_ℓ is the energy of the charged lepton, in case of charge-exchange reactions.

In eq. (4), M_J, L_J, T_J^{el} and T_J^{mag} are Coulomb, longitudinal, transverse electric and magnetic multipole operators for vector and axial-vector currents defined by

$$\begin{aligned} \langle \vec{p}' | J_\mu | \vec{p} \rangle &= i\bar{u}(\vec{p}') [F_1^V \gamma_\mu + F_2^V \sigma_{\mu\nu} q_\nu] \tau_\mp u(\vec{p}) \\ \langle \vec{p}' | J_\mu^5 | \vec{p} \rangle &= i\bar{u}(\vec{p}') [F_A \gamma_5 \gamma_\mu - iF_P \gamma_5 q_\mu] \tau_\mp u(\vec{p}) \end{aligned} \quad (5)$$

for (ν, ℓ^-) and $(\bar{\nu}, \ell^+)$ reactions. Their matrix elements

TABLE I: Cross sections for the exclusive reaction $^{12}\text{C}(\nu_e, e^-)^{12}\text{N}(1^+_{g.s.})$ obtained for DAR neutrinos by shell model calculations. The bare g_A is used except for the SFO Hamiltonian case with the value of g_A^{eff} specified as $g_A^{eff} = 0.95 g_A$. Experimental values are taken from refs. [17] and [18]. The first error is statistical and the second is systematic.

Hamiltonian	cross section ($\times 10^{-42} \text{ cm}^2$)
SFO	9.96
SFO ($g_A^{eff} = 0.95 g_A$)	9.06
PSDMK2	8.48
WBT [4]	8.42
Hayes-Towner [5]	8.40
experiment (LSND [17])	$8.9 \pm 0.3 \pm 0.9$
experiment (KARMEN [18])	$9.1 \pm 0.5 \pm 0.8$

TABLE II: Cross sections for the exclusive neutral current reaction on ^{12}C leading to the 1^+ ($T=1$, 15.1 MeV) state induced by DAR neutrinos; ν_e 's and $\bar{\nu}_\mu$'s from μ^+ decay as well as ν_μ 's from π^+ decay. Experimental values of the sum of ν_e - and $\bar{\nu}_\mu$ -induced reaction cross sections and that of ν_μ -induced reaction cross section are taken from refs. [18] and [21], respectively.

Hamiltonian	cross sections ($\times 10^{-42} \text{ cm}^2$)			
	(ν_e, ν'_e)	$(\bar{\nu}_\mu, \bar{\nu}'_\mu)$	$(\nu_e, \nu'_e) + (\bar{\nu}_\mu, \bar{\nu}'_\mu)$	(ν_μ, ν'_μ)
SFO ($g_A^{eff} = 0.95 g_A$)	4.44	5.32	9.76	2.68
PSDMK2	3.75	4.52	8.27	2.26
experiment (KARMEN)			$10.4 \pm 1.0 \pm 0.9$ [18]	$3.2 \pm 0.5 \pm 0.4$ [21]

are given in ref.[13]. F_1^V and F_2^V are isovector electromagnetic form factors, F_A is the axial-vector form factor with $F_A(q_\mu^2=0) = g_A$, and F_P is the induced pseudoscalar form factor. Here, we consider vanishing scalar and tensor couplings. In the extreme relativistic limit, when the lepton mass can be neglected, the pseudoscalar coupling in the axial-vector current does not contribute to the neutrino reaction cross sections[13]. The induced pseudoscalar terms, therefore, can be safely neglected in the present calculations, where only electrons and positrons are treated except for neutrinos as the leptons and neutrino energies are high enough compared to the electron mass.

Eq. (4) with the multipole operators obtained for the neutral current,

$$J_\mu^N = J_\mu^{A3} + J_\mu^{V3} - 2\sin^2\theta_W J_\mu^\gamma \quad (6)$$

with

$$\begin{aligned} J_\mu^\gamma &= J_\mu^S + J_\mu^{V3} \\ J_\mu^{A3} &= i\bar{u}(\vec{p}') [F_A \gamma_5 \gamma_\mu - iF_P \gamma_5 q_\mu] \frac{\tau_3}{2} u(\vec{p}) \\ J_\mu^{V3} &= i\bar{u}(\vec{p}') [F_1^V \gamma_\mu + F_2^V \sigma_{\mu\nu} q_\nu] \frac{\tau_3}{2} u(\vec{p}) \\ J_\mu^S &= i\bar{u}(\vec{p}') [F_1^S \gamma_\mu + F_2^S \sigma_{\mu\nu} q_\nu] \frac{1}{2} u(\vec{p}), \end{aligned} \quad (7)$$

applies also to (ν, ν') and $(\bar{\nu}, \bar{\nu}')$ reactions. Here, θ_W is the Weinberg angle, and F_1^S and F_2^S are isoscalar electromagnetic form factors. As mentioned above, the contributions from the pseudoscalar coupling (F_P) vanish.

First, we show results of cross sections for the exclusive reaction $^{12}\text{C}(\nu_e, e^-)^{12}\text{N}(1^+_{g.s.})$ induced by DAR neutrinos. Calculated cross sections obtained by using the SFO and the PSDMK2 [1, 15, 16] shell model Hamiltonians within the configuration space including up to $2\hbar\omega$

excitations are given in Table I as well as the observed values [17, 18]. Harmonic oscillator wave functions with a size parameter $b = 1.64$ fm are used. The axial electric dipole (E_51) and the magnetic dipole ($M1$) terms contribute to the Gamow-Teller transition. There are also contributions from the axial Coulomb and longitudinal dipole (C_51 and L_51) terms, but they are rather small. The bare axial vector coupling constant, $g_A = -1.263$ and an effective one with $g_A^{eff} = 0.95 g_A$ are used. The latter one reproduces the experimental $B(GT)$ value for the transition to $^{12}\text{N}(1^+_{g.s.})$. While the SFO Hamiltonian gives larger values of the cross section than those obtained by other conventional shell model Hamiltonians [4, 5], the calculated cross sections are found to be consistent with the experimental ones within the experimental errors [17, 18]. A no core shell model (NCSM) calculation gives a smaller value of $6.80 \times 10^{-42} \text{ cm}^2$ for the cross section [19], while a continuum random phase approximation (CRPA) method gives a larger value of $13.88 \times 10^{-42} \text{ cm}^2$ [20].

Next, we show in Table II calculated results of the cross sections for exclusive neutral current reactions on ^{12}C , that is, (ν_e, ν'_e) , $(\bar{\nu}_\mu, \bar{\nu}'_\mu)$ and (ν_μ, ν'_μ) reactions leading to the 1^+ ($T=1$, 15.1 MeV) state of ^{12}C induced by the DAR neutrinos. Experimental value of the cross section for the sum of the (ν_e, ν'_e) and $(\bar{\nu}_\mu, \bar{\nu}'_\mu)$ reactions is available [18] (see Table II). The calculated cross section obtained for the SFO Hamiltonian is found to be close to the observed value, while that for the PSDMK2 Hamiltonian is smaller than the experimental one about by 20%. Note that the $B(GT)$ value obtained for the PSDMK2 Hamiltonian with the $0-2 \hbar\omega$ configuration space is smaller than the observed one by 16% [1]. Experimental value of the (ν_μ, ν'_μ) reaction cross section [21] is also found to be consistent with the calculated value for the

TABLE III: Cross sections for the reaction process $^{12}\text{C}(\nu_e, e^-)^{12}\text{N}^*$ obtained for DAR neutrinos by shell model calculations. The bare g_A is used unless specified. Experimental values are taken from refs. [17] and [22].

Hamiltonian	cross section ($\times 10^{-42} \text{ cm}^2$)
SFO	8.35
SFO ($g_A^{eff} = 0.70g_A$)	5.22
PSDMK2	7.14
PSDMK2 ($g_A^{eff} = 0.75g_A$)	4.87
WBT [4]	8.31
Hayes-Towner [5]	3.80
experiment (LSND [17])	$4.3 \pm 0.4 \pm 0.6$
experiment (KARMEN [22])	$5.1 \pm 0.6 \pm 0.5$

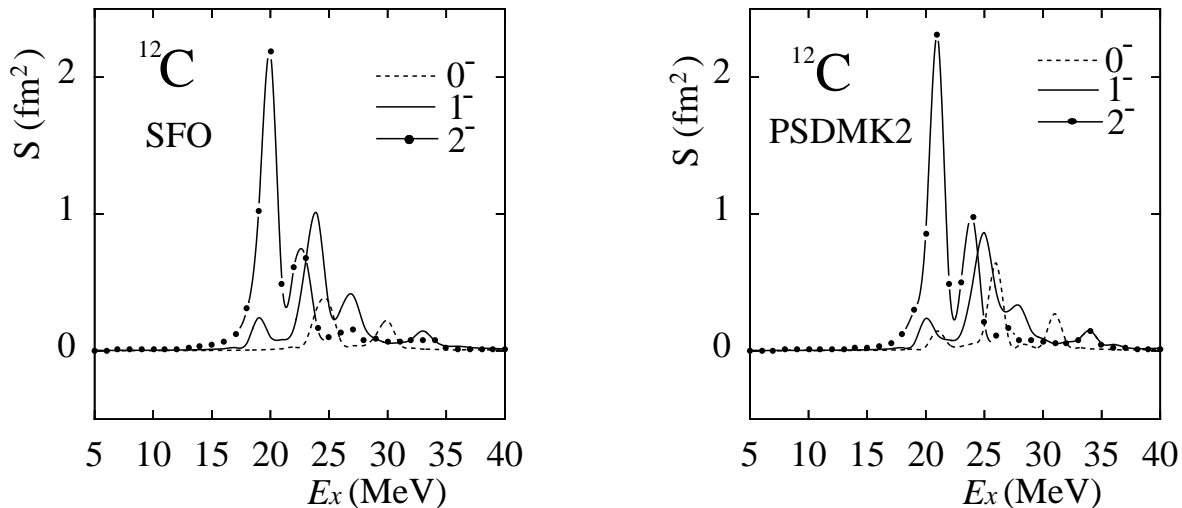


FIG. 3: Spin-dipole strengths in ^{12}C for the SFO and PSDMK2 Hamiltonians. The strengths are folded by a Lorentzian with the width of 1 MeV.

SFO Hamiltonian whereas it is a bit larger than the calculated value for the PSDMK2 Hamiltonian.

Finally, we show in Table III calculated results of the cross section for $^{12}\text{C}(\nu_e, e^-)^{12}\text{N}^*$ reaction leading to excited states of ^{12}N obtained by the shell models with the configuration space including up to $3\hbar\omega$ excitations. The multiplicities up to $J=3$ are included here. The contributions from the spin-dipole transitions to the 0^- , 1^- and 2^- states are dominant. There are also some contributions from other multiplicities, 2^+ , 3^- , 3^+ and 0^+ as well as 1^+ except for the ground state. The SFO Hamiltonian gives closer energy levels for the negative parity states than the PSDMK2 Hamiltonian. The excitation energies of the first 0^- , 1^- , 2^- and 3^- states with $T=1$ are 20.304 (21.086) MeV, 19.053 (20.137) MeV, 17.823 (18.881) MeV and 19.087 (20.128) MeV, respectively, for the SFO (PSDMK2) case, while experimental values are 17.230 MeV (1^-), 16.570 MeV (2^-) and 18.350 MeV (3^-). The spin dipole strengths obtained by the SFO and PSDMK2 Hamiltonians are shown in Fig. 3. Calculated strengths summed up to the excitation energy of

$E_x = 50$ MeV are 1.79 (1.78) fm^2 , 4.33 (4.12) fm^2 and 7.19 (7.03) fm^2 for the 0^- , 1^- and 2^- states, respectively, for the SFO (PSDMK2) Hamiltonian. The centroid energies defined by the energy-weighted sum divided by the non-energy-weighted sum of the strength are calculated to be 25.9 (26.8) MeV, 25.3 (26.2) MeV and 21.5 (22.7) MeV for the SFO (PSDMK2) case for the 0^- , 1^- and 2^- states, respectively. The strength by the SFO Hamiltonian is shifted toward lower energy region by about 1 MeV compared to the PSDMK2 Hamiltonian while the total strength is increased only about by 3%.

Shell model calculations give larger cross sections than the observed values [17, 22] except for one by Hayes and Towner [5] where Woods-Saxon wave functions are used instead of harmonic oscillator wave functions. A CRPA calculation [20] gives a cross section close to the experiment. Effective axial-vector coupling constants with quenching factors, $g_A^{eff}/g_A = 0.7$ and 0.75, are adopted for the SFO and PSDMK2 Hamiltonians, respectively. Shell model calculations with these quenching factors reproduce the experimental cross section.

There is an observational indication from electron scattering and (p, n) reaction data that the spin-dipole strength in the 2^- ($T=1$) state in ^{12}C (^{12}N) at $E_x = 19.40$ (4.14) MeV is considerably quenched by a factor of about 2 [23, 24, 25]. Note that the 2^- state exhausts about 60% of the total spin-dipole strength for 2^- states (see also ref. [25]). This results in more importance of the 2^- state in the cross section, that is, about 75% of the cross section for $^{12}\text{C} (\nu_e, e^-) ^{12}\text{N}^* (2^-)$ induced by DAR neutrinos comes from the 2^- state at 4.14 MeV due to the neutrino energy cut-off at 52.8 MeV. The $M2$ form factor for $^{12}\text{C} (e, e') ^{12}\text{C} (2^-, T=1, 19.40 \text{ MeV})$ was obtained in the momentum transfer region of $q = 0.3 \sim 1.0 \text{ fm}^{-1}$ [23]. The observed form factor is found to be consistent with a large quenching of the spin g factor: $g_s^{eff}/g_s = 0.70 \pm 0.05$ (0.75 ± 0.05) for the SFO (PSDMK2) hamiltonian. This was also pointed out in ref. [25], where $g_s^{eff}/g_s = 0.65$ was obtained for the Cohen-Kurath Hamiltonian. The (p, n) and $(d, ^2\text{He})$ reaction data support similar order of large quenching factors [24, 25, 26]. More experimental investigation is important and necessary to get systematic information on the nature of quenching of the spin-dipole strength. Quenching due to the coupling to many-particle many-hole states at high excitation energies could be larger for the spin-dipole states which lie above the Gamow-Teller state because of smaller energy-difference denominator.

In case of 2^+ ($T=1$) state, (p, n) and (p, p') reaction data indicate that the transition strength to the 2^+ ($T=1$) state in ^{12}N (^{12}C) at $E_x = 0.96$ (16.11) MeV is quenched by a factor of about 2 [27, 28]. It was also found in ref. [29] that in the electric dipole transitions in ^{12}C the reduction of the calculated cross section by a multiplying factor of 0.7 was necessary in order to obtain quantitative agreement with the available experimental cross section [30]. This suggests the importance of the coupling to many-particle many-hole states with excitations larger than $3\hbar\omega$. We thus get several supports from observations for the necessity for the large quenching of g_A in the inclusive reactions.

B. REACTIONS ON ^{12}C INDUCED BY SUPERNOVA NEUTRINOS

We study charge-exchange and neutral current reactions on ^{12}C induced by the supernova neutrinos. Fermi distribution functions are employed for the spectra of the supernova neutrinos. The value of the chemical potential is set to be zero. Average energies of supernova neutrinos are about 10 MeV, 15 MeV and $15 \sim 25$ MeV for ν_e , $\bar{\nu}_e$, ν_μ and ν_τ , respectively [31]. The neutrino temperature of the Fermi distribution is about one-third of the average energy.

Calculated cross sections for supernova neutrinos with temperature $T = 2 \sim 12$ MeV are shown in Fig. 4 for the SFO and PSDMK2 Hamiltonians. The axial-vector coupling constants which reproduce the experimental

(ν_e, e^-) cross section for the DAR neutrinos are adopted. The values of g_A^{eff}/g_A are 0.95 and 0.70 for the exclusive reaction and the transitions to the excited states, respectively, in case of the SFO Hamiltonian. Those employed for the PSDMK2 Hamiltonian are 1.0 for the exclusive reaction and 0.75 for the transitions to the excited states, respectively. We will use these values for g_A^{eff} hereafter. As for the neutral current reactions, contributions from the isoscalar transitions are not included in the calculations as they are quite small. Calculated cross sections for the SFO are enhanced compared with those for the PSDMK2 in both charge-exchange and neutral current reactions. The charge-exchange reaction cross sections are also enhanced compared with the previous calculations by Woosley et al.[6], in which the configurations are restricted to up to $1\hbar\omega$ excitations with $g_A^{eff}/g_A = 0.7$ for the excitations of the negative-parity states.

Branching ratios from each excited level are calculated for decay channels involving neutron, proton, α and γ by the Hauser-Feshbach statistical model [32]. All the levels obtained by the present shell model calculations are adopted as levels in the decaying and daughter nuclei with specific isospin assignments.

The particle transmission coefficients are calculated by the optical model with conventional potentials [33, 34] at selected grid energies, and they are interpolated by using a spline interpolation. Weights proportional to the square of the isospin CG-coefficients are multiplied to the transmission coefficients obtained by the optical model to account for the isospin conservation. We ignored any isospin mixing which may be significant for some of the light nuclei. The γ -transmission coefficients are calculated with a simple Brink's formula. The E1 and M1 parameters were taken from RIPL-2 database [35]. The γ -cascade in the initial excited nuclei and subsequent decay were fully considered.

Calculated branching ratios as well as the proton and neutron emission cross sections are shown in Fig. 5 for the neutral current reactions. The branching ratios for the proton and neutron emissions obtained by the PSDMK2 Hamiltonian are close to those of ref. [6]. The branching ratios for the proton emissions depend on the Hamiltonians, SFO or PSDMK2, while the neutron emission cross sections are found to be enhanced for the SFO case.

Neutral current reactions, $^{12}\text{C} (\nu, \nu'p) ^{11}\text{B}$ and $^{12}\text{C} (\nu, \nu'n) ^{11}\text{C} (\beta^+) ^{11}\text{B}$, are important for the production of ^{11}B in the He-C layer and O-rich layer during supernova explosions. The effects of the reactions on the abundance of ^{11}B in the supernovae will be discussed in sect. IV.

C. REACTIONS ON ^4He

We treat here the ^4He nucleus for the study of neutrino-nucleus reactions. The reaction cross sections on the nucleus has an important role in determining

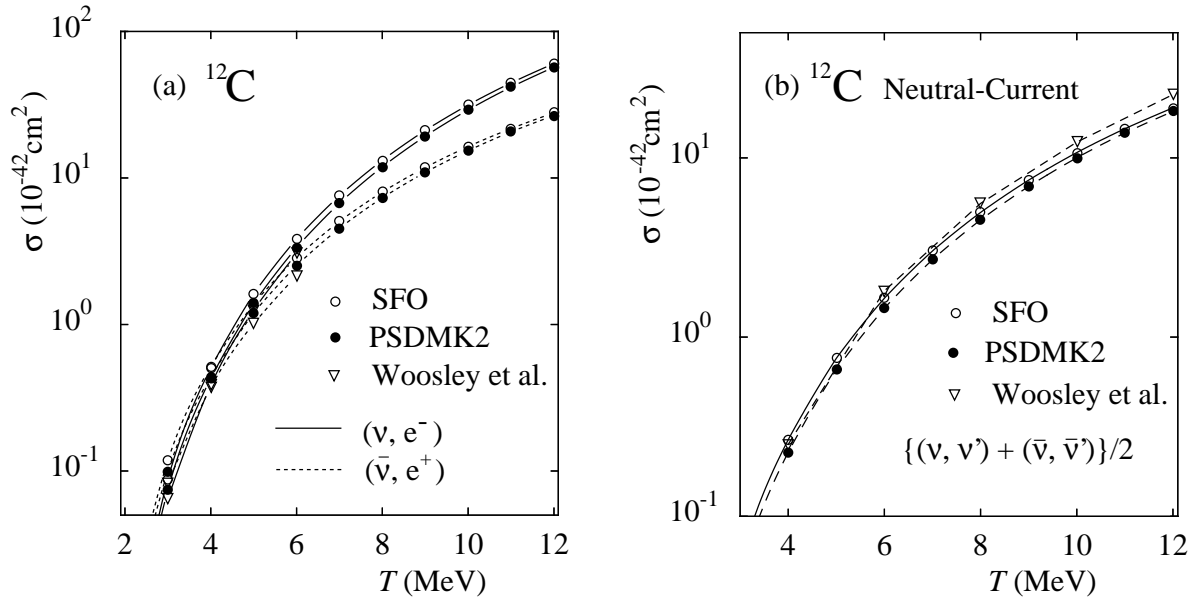


FIG. 4: Calculated cross sections for neutrino ^{12}C reactions induced by supernova neutrinos with temperature T obtained by using the SFO and PSDMK2 Hamiltonians. Both (a) the charge-exchange (ν_e, e^-) and $(\bar{\nu}_e, e^+)$ reactions, and (b) the neutral current reactions are treated. Average values of the (ν, ν') and $(\bar{\nu}, \bar{\nu}')$ cross sections are shown for the neutral current reactions. Previous calculations of ref. [6] are also given.

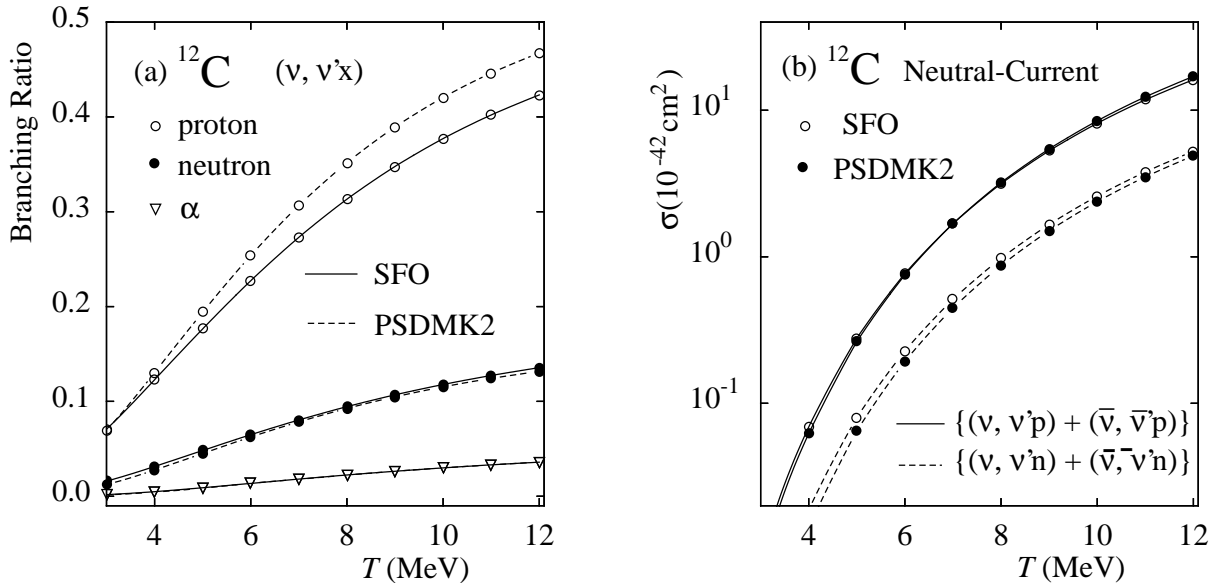


FIG. 5: (a) Branching ratios for proton, neutron and α emission channels for neutral current reactions on ^{12}C obtained by the Hauser-Feshbach theory. (b) Calculated cross sections for proton and neutron knock-out channels obtained by using the SFO and PSDMK2 Hamiltonians.

abundances of light elements such as ^7Li and ^{11}B during supernova explosions.

The ν - ^4He reactions are induced dominantly by excitations of spin-dipole states. The Warburton-Brown (WBP) [36] and Millener-Kurath (SPSDMK) [15, 16]

Hamiltonians are used for the shell model calculations of ^4He with configurations including up to $3\hbar\omega$ excitations. In the SPSDMK interaction, the Cohen-Kurath interaction, (8-16)POT [7], is used for the p -shell part while the Millener-Kurath interaction is used for the cross-shell

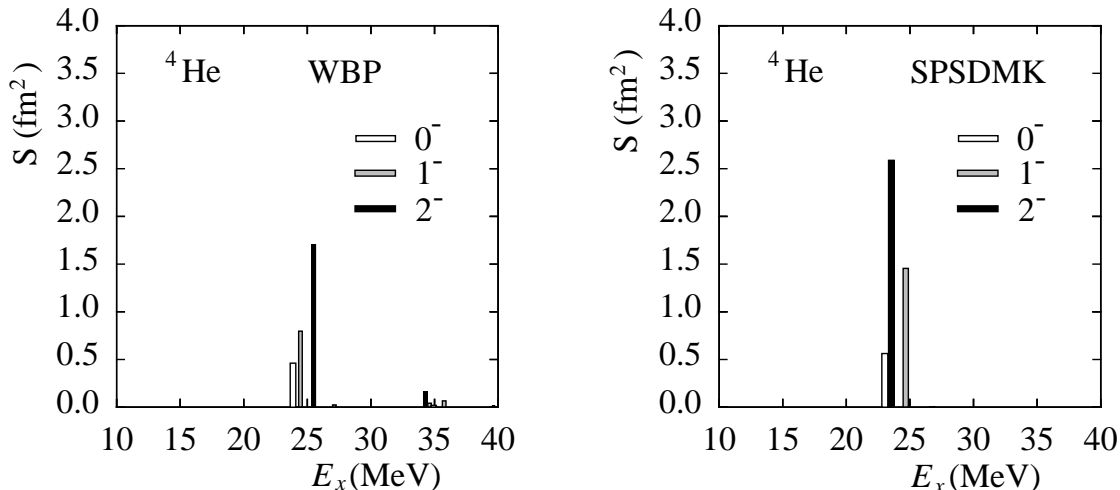


FIG. 6: Spin-dipole strengths in ${}^4\text{He}$ for the WBP and SPSDMK Hamiltonians

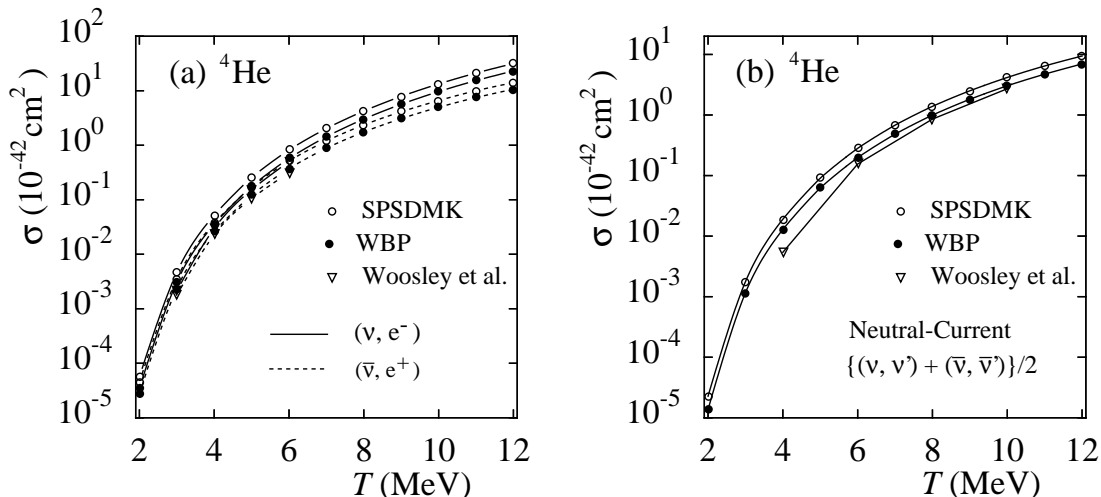


FIG. 7: Calculated (a) charge-exchange and (b) neutral current reaction cross sections for ν - ${}^4\text{He}$ reactions obtained by using the WBP and SPSDMK Hamiltonians. Previous calculations of ref. [6] are also shown.

matrix elements between $0s$ and $0p$ as well as $0p$ and $1s0d$ orbits. The sd -shell part is the Freedom-Wildenthal interaction [37], and all others are Kuo's renormalized G-matrices [38].

Calculated spin-dipole strengths are shown in Fig. 6. Harmonic oscillator wave functions with a size parameter $b = 1.38$ fm are used. The strength is more fragmented in the case of the WBP Hamiltonian. The summed strengths are 3.34 fm 2 for the WBP and 4.71 fm 2 for the SPSDMK Hamiltonians, respectively, up to the excitation energy of $E_x = 50$ MeV.

Calculated cross sections for the charge-exchange and neutral current reactions are shown in Fig. 7 for the supernova neutrinos with $T = 2 \sim 12$ MeV. The bare g_A is employed. The cross sections for the SPSDMK case are

found to be larger than those for the WBP case. They are both enhanced compared to the previous calculations [6], where Sussex matrix elements [9] are used for the effective interaction with a larger harmonic oscillator size parameter of $b = 1.5$ fm.

A recent microscopic *ab initio* calculation of the neutral current reaction on ${}^4\text{He}$ with a realistic nucleon-nucleon interaction, $AV8'$ [39], predicts cross sections with a steeper dependence on the neutrino temperature than the shell model calculations [40]. At $T = 10$ MeV, the calculated cross section in ref. [40] is close to that obtained by the WBP Hamiltonian, while at $T = 12$ MeV it is enhanced by about 16%. At $T = 8$ MeV, on the other hand, the WBP Hamiltonian predicts a larger cross section by about 15%.

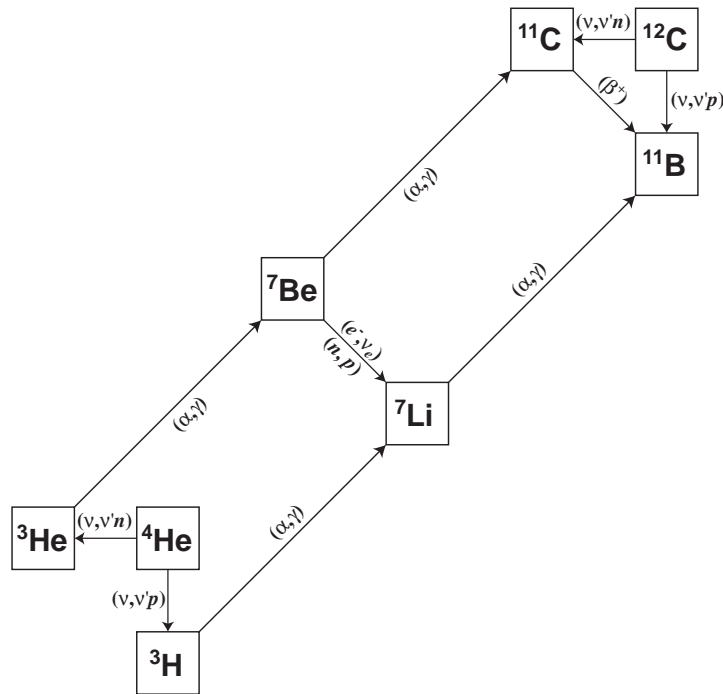


FIG. 8: Nucleosynthesis path of light elements ${}^7\text{Li}$ and ${}^{11}\text{B}$ during supernova explosions.

The neutral current reactions, ${}^4\text{He}(\nu, \nu'p){}^3\text{H}$ and ${}^4\text{He}(\nu, \nu'n){}^3\text{He}$, are important for the production of ${}^7\text{Li}$ through ${}^3\text{H}(\alpha, \gamma){}^7\text{Li}$ and ${}^3\text{He}(\alpha, \gamma){}^7\text{Be}(e^-, \nu_e){}^7\text{Li}$ processes in the He-C layer during supernova explosions. The reactions are also important for the production of ${}^{11}\text{B}$ as the abundance of ${}^7\text{Li}$ affects the production of ${}^{11}\text{B}$ through the process ${}^7\text{Li}(\alpha, \gamma){}^{11}\text{B}$.

IV. ABUNDANCES OF ${}^7\text{Li}$ AND ${}^{11}\text{B}$ DURING SUPERNOVA EXPLOSIONS

The enhancement of ν - ${}^4\text{He}$ and ν - ${}^{12}\text{C}$ reaction cross sections affects the abundances of ${}^7\text{Li}$ and ${}^{11}\text{B}$ in the nucleosynthesis process during supernova explosions. The nucleosynthesis path of light elements is shown in Fig. 8. The neutral current reactions, ${}^{12}\text{C}(\nu, \nu'p){}^{11}\text{B}$ and ${}^{12}\text{C}(\nu, \nu'n){}^{11}\text{C}$, are important for the production of ${}^{11}\text{B}$. If these cross sections are enhanced, the abundance of ${}^{11}\text{B}$ is increased. The reactions, ${}^4\text{He}(\nu, \nu'p){}^3\text{H}$ and ${}^4\text{He}(\nu, \nu'n){}^3\text{He}$ are important for the production of ${}^7\text{Li}$ through ${}^3\text{H}(\alpha, \gamma){}^7\text{Li}$ and ${}^3\text{He}(\alpha, \gamma){}^7\text{Be}(e^-, \nu_e){}^7\text{Li}$ processes. If the ν - ${}^4\text{He}$ reaction cross sections are enhanced, the abundances of both ${}^7\text{Li}$ and ${}^{11}\text{B}$ are increased as the abundance of ${}^{11}\text{B}$ is affected by that of ${}^7\text{Li}$ through ${}^7\text{Li}(\alpha, \gamma){}^{11}\text{B}$ etc.

In order to investigate the effects of our new reaction cross sections for ν - ${}^4\text{He}$ and ν - ${}^{12}\text{C}$ on the yields of ${}^7\text{Li}$ and ${}^{11}\text{B}$ in a core-collapse supernova, we carry out detailed nucleosynthesis calculation during supernova explosions. The supernova explosion model is the same as in [41, 42]. The progenitor structure is adopted from a

$16.2 M_{\odot}$ presupernova model corresponding to SN 1987A [43]. The nuclear reaction network consists of 291 species of nuclei. The luminosity and energy spectra of neutrinos are important for neutrino-nucleus interactions. We assume that the neutrino luminosity decays exponentially in time with a time scale of 3 s and is equally partitioned among three flavors of neutrinos and antineutrinos. The neutrino energy spectra are assumed to obey Fermi distributions with zero-chemical potentials. We set the total neutrino energy to be 3×10^{53} erg and the neutrino temperatures of ν_e , $\bar{\nu}_e$, and $\nu_{\mu, \tau}$ and $\bar{\nu}_{\mu, \tau}$ to be $T_{\nu_e} = 3.2$ MeV, $T_{\bar{\nu}_e} = 5.0$ MeV, and $T_{\nu_{\mu, \tau}} = 6.0$ MeV, respectively [41, 42], as the standard case.

We show in Table IV production yields of ${}^7\text{Li}$ and ${}^{11}\text{B}$ in the nucleosynthesis during the supernova explosion obtained by using the cross sections of the two sets of the shell model Hamiltonians; one by WBP for ${}^4\text{He}$ and SFO for ${}^{12}\text{C}$ and the other by SPSPDMK for ${}^4\text{He}$ and PS-DMK2 for ${}^{12}\text{C}$. The production yields obtained by using the cross sections of Hoffman and Woosley (HW92) [44] are also given. Compared to the case by HW92, the abundances of ${}^7\text{Li}$ and ${}^{11}\text{B}$ are enhanced by a factor of 1.30 and 1.19, respectively, for WBP+SFO, while they are enhanced more by a factor of 1.79 and 1.49, respectively, for SPSPDMK+PSDMK2. Enhancement factors for ${}^7\text{Li}$ are larger than those for ${}^{11}\text{B}$, which comes from the fact that the cross sections for ${}^4\text{He}$ are more enhanced than those for ${}^{12}\text{C}$. We find that about 40% of the production of ${}^{11}\text{B}$ is caused by the ν - ${}^{12}\text{C}$ reactions while the other 60% is due to the ν - ${}^4\text{He}$ reactions.

We investigate the production yields of ${}^7\text{Li}$ and ${}^{11}\text{B}$ by changing the temperature of ν_e , $\bar{\nu}_e$, and $\nu_{\mu, \tau}$. We set the

TABLE IV: Production yields of ${}^7\text{Li}$ and ${}^{11}\text{B}$ in a supernova explosion model

Hamiltonians	$M({}^7\text{Li})/M_\odot$	$M({}^{11}\text{B})/M_\odot$
WBP + SFO	3.06×10^{-7}	7.51×10^{-7}
SPSDMK + PSDMK2	4.24×10^{-7}	9.38×10^{-7}
HW92	2.36×10^{-7}	6.29×10^{-7}

TABLE V: Dependence of the production yields of ${}^7\text{Li}$ and ${}^{11}\text{B}$ on neutrino temperatures and total neutrino energy. Reaction cross sections by (a) WBP and SFO Hamiltonians as well as (b) PSDMK and PSDMK2 Hamiltonians for ${}^4\text{He}$ and ${}^{12}\text{C}$, respectively, are used.

Hamiltonians	Neutrino model	T_{ν_e} (MeV)	$T_{\bar{\nu}_e}$ (MeV)	$T_{\nu_{\mu,\tau}}$ (MeV)	E_ν ($\times 10^{53}$ erg)	$M({}^7\text{Li})$ (M_\odot)	$M({}^{11}\text{B})$ (M_\odot)
(a) WBP + SFO	Low T_ν , High E_ν	3.2	4.1	5.0	3.53	1.51×10^{-7}	3.59×10^{-7}
	Med T_ν , Med E_ν	3.2	4.8	5.8	3.0	2.62×10^{-7}	6.36×10^{-7}
	High T_ν , Low E_ν	3.2	5.0	6.4	2.35	3.13×10^{-7}	7.45×10^{-7}
(b) PSDMK + PSDMK2	Low T_ν , High E_ν	3.2	4.0	4.8	3.53	1.76×10^{-7}	3.55×10^{-7}
	Med T_ν , Med E_ν	3.2	4.6	5.6	3.0	3.07×10^{-7}	6.57×10^{-7}
	High T_ν , Low E_ν	3.2	5.0	6.0	2.35	3.41×10^{-7}	7.35×10^{-7}

following restrictions to the temperature; (1) $T_{\nu_e} < T_{\bar{\nu}_e} < T_{\nu_{\mu,\tau}}$, (2) $T_{\bar{\nu}_e} \leq 5$ MeV, and (3) $T_{\nu_{\mu,\tau}}/T_{\bar{\nu}_e} \simeq 1.2$. We further choose temperature so that the production yield of ${}^{11}\text{B}$ ranges between $3.3 \times 10^{-7} M_\odot$ and $7.4 \times 10^{-7} M_\odot$ in order to satisfy the supernova contribution of B abundance in the Galactic chemical evolution [42, 45]. The total neutrino energy is varied within the estimated error bar for the released gravitational binding energy of a proto-neutron star [46]. Calculated results are given in Table V. Although the production yield of ${}^{11}\text{B}$ depends little on the Hamiltonians, the production yield of ${}^7\text{Li}$ is slightly larger for the case of PSDMK+PSDMK2 compared with the case of WBP+SFO.

When we take into account the effect of neutrino oscillations, charge-exchange reactions make an additional role to increase both ${}^7\text{Li}$ and ${}^{11}\text{B}$ yields. The production yields prove to be sensitive to the mixing angles, in particular to θ_{13} , and mass hierarchy [41]. This subject with the use of our new reaction cross sections will be discussed in ref. [47].

V. SUMMARY

Neutrino-nucleus reactions on ${}^{12}\text{C}$ induced by DAR neutrinos and supernova neutrinos are investigated by using a new shell model Hamiltonian for p -shell nuclei, SFO, which takes into account important roles of spin-isospin interactions.

First, the monopole terms of the tensor components of the SFO interaction are shown to have proper signs, that is, the p-n interaction is attractive between j_j and j_l orbits but repulsive between j_j and j_j or j_l and j_l orbits. This zigzag structure of the tensor interaction is pointed out to be important to realize the proper evolution of effective single particle energies toward the drip-lines. For

$N=8$ isotones, the shell gap between the $0p_{1/2}$ and $0p_{3/2}$ orbits is shown to increase near the neutron-rich side.

Cross sections of charge-exchange exclusive and inclusive reactions on ${}^{12}\text{C}$ are, then, obtained for the DAR neutrinos with the use of the SFO Hamiltonian, and compared with experimental values. The exclusive reaction is found to be well reproduced with $g_A^{eff} = 0.95 g_A$. A quenching of g_A ($g_A^{eff} = 0.7 g_A$) is found to be necessary to explain the cross section for excited states.

Charge-exchange and neutral current reactions are studied also for supernova neutrinos. Branching ratios to proton, neutron, α and γ emission channels are calculated by the Hauser-Feshbach theory, and cross sections for $(\nu, \nu'p)$ and $(\nu, \nu'n)$ reactions are obtained. Calculated cross sections are found to be enhanced compared to those by the PSDMK2 Hamiltonian.

Neutrino- ${}^4\text{He}$ reactions are also investigated by using the WBP and the PSDMK Hamiltonians. Calculated cross sections are enhanced compared with previous calculations of ref. [6]. A possible consequence of the enhancement of the ν - ${}^4\text{He}$ and ν - ${}^{12}\text{C}$ reaction cross sections on the abundances of light elements is discussed. The production yields of ${}^7\text{Li}$ and ${}^{11}\text{B}$ are found to be enhanced during supernova explosions.

Acknowledgements

This work has been supported in part by Grants-in-Aid for Scientific Research (14540271, 17540275, 18540290) and for Specially Promoted Research (13002001) of the Ministry of Education, Culture, Sports, Science and Technology of Japan, and Mitsubishi Foundation. The authors would like to thank Professor A. Gelberg for the careful reading of the manuscript.

-
- [1] T. Suzuki, R. Fujimoto, and T. Otsuka, Phys. Rev. C **67**, 044302 (2003).
- [2] T. Otsuka, R. Fujimoto, Y. Utsuno, B. A. Brown, M. Honma, and T. Mizusaki, Phys. Rev. Lett. **87**, 082502 (2001).
- [3] T. Otsuka, T. Suzuki, R. Fujimoto, H. Grawe, and Y. Akaishi, Phys. Rev. Lett. **95**, 232502 (2005).
- [4] C. Volpe, N. Auerbach, G. Colò, T. Suzuki, and N. Van Giai, Phys. Rev. C **62**, 015501 (2000).
- [5] A. C. Hayes and I. S. Towner, Phys. Rev. C **61**, 044603 (2000).
- [6] S. E. Woosley, D. H. Hartmann, R. D. Hoffman, and W. C. Haxton, Astrophys. J. **356**, 272 (1990).
- [7] S. Cohen and D. Kurath, Nucl. Phys. **73**, 1 (1965).
- [8] M. W. Kirson, Phys. Lett. B **47**, 110 (1973);
I. Kakkar and Y. R. Waghmare, Phys. Rev. C **2**, 1191 (1970);
K. Klingenberg, W. Knüpfer, M. G. Huber, and P. W. M. Glaudemans, Phys. Rev. **C15**, 1483 (1977).
- [9] J. P. Elliott, A. D. Jackson, H. A. Mavromatis, E. A. Sanderson, and B. Singh, Nucl. Phys. **A121**, 241 (1968).
- [10] F. Osterfeld, Rev. Mod. Phys. **64**, 491 (1992);
S. -O. Bäckman, G. E. Brown, and J. A. Niskanen, Phys. Rep. **124**, 1 (1985).
- [11] G. Bertsch, J. Borysowicz, H. McManus, and W. G. Love, Nucl. Phys. **A284**, 399 (1977).
- [12] R. E. McDonald, J. A. Becker, R. A. Chalmers, and D. H. Wilkinson, Phys. Rev. C **10**, 333 (1974).
- [13] J. D. Walecka, in *Muon Physics*, edited by V. H. Hughes and C. S. Wu (Academic, New York, 1975), Vol. II;
J. S. O'Connell, T. W. Donnelly, and J. D. Walecka, Phys. Rev. C **6**, 719 (1972);
T. W. Donnelly and J. D. Walecka, Nucl. Phys. **A274**, 368 (1976);
T. W. Donnelly and W. C. Haxton, Atomic Data Nucl. Data Tables **23**, 103 (1979).
- [14] D. H. Wilkinson and B. E. F. Macefield, Nucl. Phys. **A232**, 58 (1974).
- [15] OXBASH, The Oxford, Buenos-Aires, Michigan State, Shell Model Program, B. A. Brown, A. Etchegoyen, and W. D. M. Rae, MSU Cyclotron Laboratory Report No. 524, 1986.
- [16] D. J. Millener and D. Kurath, Nucl. Phys. **A255**, 315 (1975).
- [17] LSND Collaborations, L. B. Auerbach et al., Phys. Rev. C **64**, 065501 (2001).
- [18] KARMEN Collaboration, B. E. Bodmann et al., Phys. Lett. B **332**, 251 (1994).
- [19] A. C. Hayes, P. Navrátil, and J. P. Vary, Phys. Rev. Lett. **91**, 12502 (2003).
- [20] E. Kolb, K. Langanke, and P. Vogel, Nucl. Phys. **A652**, 91 (1999).
- [21] KARMEN Collaboration, B. A. Armbruster et al., Phys. Lett. B **423**, 15 (1998).
- [22] R. Maschuw, Prog. Part. Nucl. Phys. **40**, 183 (1998).
- [23] T. E. Drake, E. L. Tomusiak and H. S. Caplan, Nucl. Phys. **A118**, 138 (1968);
A. Yamaguchi, T. Terasawa, K. Nakahara and Y. Torizuka, Phys. Rev. C **3**, 1750 (1971).
- [24] X. Yang et al., Phys. Rev. C **48**, 1158 (1993).
- [25] C. Gaarde et al., Nucl. Phys. **A422**, 189 (1984).
- [26] H. Okamura et al., Phys. Lett. B **345**, 1 (1995).
- [27] J. Rapaport, T. Taddeucci, C. Gaarde, C. D. Goodman, C. C. Foster, C. A. Goulding, D. Horen, E. Sugarbaker, T. G. Masterson and D. Lind, Phys. Rev. C **24**, 335 (1981).
- [28] J. R. Comfort, S. M. Austin, P. T. Debevec, G. L. Moake, R. W. Finlay and W. G. Love, Phys. Rev. C **21**, 2147 (1980).
- [29] T. Suzuki, H. Sagawa and K. Hagino, Phys. Rev. C **68**, 014317 (2003).
- [30] R. E. Pywell, B. L. Berman, J. G. Woodworth, J. W. Jury, K. G. McNeil and M. N. Thompson, Phys. Rev. C **32**, 384 (1985);
D. J. Mclean, M. N. Thompson, D. Zubanov, K. G. McNeil, J. W. Jury and B. L. Berman, *ibid.* **44**, 1137 (1991).
- [31] M. Th. Keil, G. G. Raffelt, and H. -Th. Janka, Astrophys. J. **590**, 971 (2003).
- [32] W. Hauser and H. Feshbach, Phys. Rev. **87**, 366 (1952).
- [33] R. L. Walter and P. P. Guss, *Proc. Int. Conf. on Nucl. Data for Basic and Applied Sci.*, Santa Fe, May 13-17, 1985, p.1079 (1986).
- [34] V. Avrigeanu and P. E. Hodgson, Phys. Rev. C **49**, 2136 (1994).
- [35] T. Belgya, O. Bersillon, R. Capote, T. Fukahori, G. Zhigang, S. Goriely, M. Herman, A. V. Ignatyuk, S. Kailas, A. Koning, P. Oblozhinsky, V. Plujko, and P. Young, "Handbook for calculations of nuclear reaction data: Reference Input Parameter Library", available online at <http://www-nds.iaea.org/RIPL-2/>, IAEA, Vienna (2005).
- [36] E. K. Warburton and B. A. Brown, Phys. Rev. C **46**, 923 (1992).
- [37] B. M. Preedom and B. H. Wildenthal, Phys. Rev. C **6**, 1633 (1972).
- [38] T. T. S. Kuo, Nucl. Phys. **A103**, 71 (1967).
- [39] B. S. Pudlinger, V. R. Pandharipande, J. Carlson, S. C. Pieper, and R. B. Wiringa, Phys. Rev. C **56**, 1720 (1997).
- [40] D. Gazit and N. Barnea, Phys. Rev. C **70**, 048801 (2004).
- [41] T. Yoshida, T. Kajino, H. Yokomakura, K. Kimura, A. Takamura, and D. H. Hartmann, Phys. Rev. Lett. **96**, 091101 (2006).
- [42] T. Yoshida, T. Kajino, and D. H. Hartmann, Phys. Rev. Lett. **94**, 231101 (2005).
- [43] T. Shigeyama and K. Nomoto, Astrophys. J. **360**, 242 (1990).
- [44] R. D. Hoffman and S. E. Woosley, Neutrino Interaction Cross Sections and Branching Ratios, http://www-phys.llnl.gov/Research/RRSN/nu_csbr/neu_rate.html, (1992).
- [45] T. Yoshida, M. Terasawa, T. Kajino, and K. Sumiyoshi, Astrophys. J. **600**, 204 (2004).
- [46] J. M. Lattimer and M. Prakash, Astrophys. J. **550**, 426 (2001).
- [47] T. Yoshida, T. Kajino, T. Suzuki, S. Chiba, T. Otsuka, A. Takamura, K. Kimura, H. Yokomakura, and D. H. Hartmann, in preparation.